Revista Argentina de Clínica Psicológica
2020, Vol. XXIX, N°4, 843-850
DOI: 10.24205/03276716.2020.891

Diagnostic Value of CT Combined with Serum CEA and CA-125 In Extra-Uterine Pelvic Leiomyomas and Ovarian Sex Cord-Stromal Tumor

Chong Yang He, Ming Wen

ABSTRACT

Uterus and ovary are the most common origin of benign and malignant pelvic tumors. Extrauterine leiomyoma and sex cord-stromal tumor have substantial overlap in clinical manifestation and imaging signs. Both ultrasonography and magnetic resonance imaging (MRI) have their intrinsic limits that are subject to enterocoel gas, spatial relationship between tumor and adjacent tissues, and dislocation of uterus. Our study investigated the value of computed tomography (CT) combined with serum CEA and CA-125 levels in the differential diagnosis of extrauterine leiomyoma and ovarian sex cord-stromal tumor. Clinical data, serum CEA and CA-125 levels of 43 patients with extrauterine leiomyoma and 36 patients with ovarian sex cord-stroma tumor were analyzed retrospectively, along with the plain and enhanced CT images. Compared with pathological ascertainment, our results showed that CEA, CA-125 levels, enhancement of mass, arterial blood supply, and presence of normal ovary, OVPS and ascites are independent factors for differentiation of extrauterine leiomyoma and sex-cord stroma tumors. A multivariate logistic regression model incorporated these variables rendered a diagnostic accuracy of 95.2% in extrauterine leiomyoma (sensitivity=93%, specificity=91.2%), and 90.8% in sex cord-stroma tumor (sensitivity=80.56%, specificity=86.2%). Our study highlighted the potential of combined use of CT signs with serum biomarker CEA and CA-125 in diagnosis of etrauterine leiomyoma and sex cord-stromal tumor which are intractably differentiated by ultrasonography and MRI.

KEYWORD: Extrauterine leiomyoma, Sex cord-stromal tumor of ovary, CA-125, Computed tomography, Miltivariate logistic model

INTRODUCTION

Uterine leiomyomas is a common condition occur in 70% of women world-wide, and 25% of them develop significant symptoms[1]. Ovary and uterus are the major source of female pelvic benign and malignant tumors. Ovarian sex cord-stromal tumors originate from stroma or sex cords, which accounts for 4.3%-6.0% ovarian cancers [2]. Patients with ovarian sex cord-stromal tumors manifest with pain in lower abdomen and bloating or an increase size of abdomen [3]. Pelvic leiomyomas are common benign tumors formed by hyperplasia of connective tissue and smooth muscle in the uterus. Extrauterine leiomyoma is a rare atypical uterine leiomyoma that arises from smooth muscle cells of vulva, ovaries, urethra, urinary bladder, GIT, and vagina, etc. It can also present mass and pain in lower abdomen[4]. Accumulated clinical evidence showed that ovarian sex cord-stromal tumors share substantial proportion of signs and imaging manifestations with large extrauterine leiomyomas[5]. Ultrasonography, magnetic resonance Imaging (MRI) and computerized tomography (CT) are widely adopted technologies to diagnosis of these diseases. However, ultrasonography can be disrupted by bowel gas and the field intensity, which limits its use in identifying the spatial relations between tumor and adjacent tissues and pelvic dislocation [6]. The effectiveness of MRI is also compromised when identifying the original locus of pelvic mass with longest diameter > 5cm [7].

Department of Radiology, the First Affiliated Hospital of Chongqing Medical University,Chongqing 400016
***Corresponding Author: Ming Wen**
Address: Radiology Department, The First Affiliated Hospital of Chongqing Medical University, Youyi Road 1, Yuzhong District, Chongqing,China
Email: liuyucun65@163.com

Protein biomarkers have been extensively assayed in various tumors, and the correlation between biomarker level in blood or tissue and the disease status are well established as noninvasive diagnostic tools being used to monitor disease progression. Multiple lines of evidence investigated serum CEA and CA-125 level in gynecological oncology [8, 9]. CEA is a broad-spectrum biomarker that is used as indicator for various malignancies [10, 11]. While CA-125 is expressed abundantly in female ovarian tissues, and its diagnostic value has been testified in different epithelial ovarian cancer subtypes[12, 13]. We postulate that combining use of serum CEA, CA-125 levels and characteristic CT signs could improve the sensitivity and specificity than them serving as single indicator. The present study was conducted to explore the combined use of these 3 assays in differentiating extrauterine leiomyomas and ovarian sex cord-stroma tumor, as an attempt to provide supporting evidences for clinical diagnosis and ascertainment of these diseases.

MATERIAL AND METHODS

Patients and data

This study conducted retrospective analysis on clinical data of patients who were admitted to The First Affiliated Hospital of Chongqing Medical University from Jan 2015 to Feb 2019. Inclusion criteria are as follows: 1) Clear and complete full abdominal CT scan and three-phase contrast-enhanced CT scans; 2) Postoperative pathologically diagnosed as extrauterine leiomyomas or ovarian sex cord-stroma tumors; 3) Longest diameter>5cm and has more than 2/3 solid components; 4) Tumors of extrauterine leiomyoma protruding beyond the uterus by more than 2/3 or are broad ligament myoma. Patients present with tumor infiltration into adjacent tissues or organs or develop distant metastasis were excluded from this study.

Finally, we recruited 43 extrauterine leiomyoma patients, 40 of which were subserosal leiomyomas, 3 were broad ligament myoma. The ages range from 18 to 80 years, with average 44.53±19.78-year-old. The average longest diameter of tumors was 9.51±3.72 cm. Twenty cases were found during health check, 9 cases were post-menopausal, 19 cases experienced abdominal pain and/or paramenia, and 4 cases were self-reported palpable mass. Of the totally 36 recruited sex cord-stroma tumor patients, there were 4 fibromas, 29 granulosa-stroma cell tumors, 3 sertoli-leydig cell tumors. The ages range from 18 to 80 years old, with average 57.73±12.34. The average longest diameter of tumors was 10.9±4.2 cm. Twenty of them were postmenopausal, 4 cases were found during health check, 23 cases experienced abdominal pain or paramenia, 4 cases experienced dysmenorrhea, 4 were self-reported palpable mass, and 1 case presented voice change and hirsutism. Clinical characteristics were summarized in Table 1.

This study has been approved by Ethic Committee of The First Affiliated Hospital of Chongqing Medical University, and all informed consent were obtained from patients.

CT acquisition

All patients underwent full abdominal plain CT scan and three-phase contrast-enhanced scan with SIEMENS dual source CT scanner SOMATOM Definition Flash. Parameters are as follows: tube voltage 100-120 kV, tube current 120-200 mAs, slice thickness 5mm, slice spacing 5mm, pitch 1. All original images were reconstructed with a slice thickness of 1mm and a slice spacing of 1mm. Patients were through routine bowel preparation before full abdominal plain CT scan, followed by contrast-enhanced CT scan at 30s, 70s and 300s after injection of iopamidol (H20053388, Bracco Sine, Shanghai) dorsal vein of the hand at 1.5mL/kg, 3.5mL/s and finally 30mL 0.9% saline flush via power injector.

CT image evaluation

Data were transferred to ADW4.5 workstation to perform post-process reconstruction, including Multiplanar Reconstruction (MPR), Maximal Intensity Projection (MIP) and Volume Reconstruction (VR), etc. Two radiologists with more than 10 years of experience in image assessment analyzed the images separately, recorded location of tumor and ureter, spatial relation between tumor supply artery, venae ovarica and tumor, Ovarian Vascular Pedicle Sign (OVPS), extent of enhancement and presence of ascetic fluid. Both radiologists were blinded to the pathological information, and discrepancies were resolved by consensus.

Statistical analysis

SPSS 17.0 software was adopted to perform statistical analysis for the data. Normally distributed data were presented as Mean±SD. Group comparison was analyzed with Student's t-test. Enumeration data was represented with frequency (%) and analyzed with Chi-square nonparametric test. Variables that were significant in univariate analysis were further testified in multivariate logistic regression. Receiver Operating

Characteristic Curve (ROC) was employed to verify the diagnostic effectiveness of our logistic prediction model, from which Area Under Curve (AUC) and cut-off values were derived. P<0.05 was considered statistically significant.

RESULTS

Comparison of preoperative CT images and signs of extrauterine leiomyoma and sex cord-stroma tumor

Extrauterine leiomyoma locates before ureter, supplied by the uterine arteries that exhibited increase thickness, bending, and branches. Those supply arteries are relatively evenly distributed within the tumor, and the solid mass is significantly enhanced (Figure 1). Sex cord-stroma tumor locates before ureter, supplied by ovarian arteries that present less branches and evenly distributed within the solid tumor. OVPS is present in venous phase, and the solid mass was slightly enhanced (Figure 2).

Compared with extrauterine leiomyomas, the solid mass of sex cord-stroma tumor was slightly enhanced, and the tumors were supplied by ovarian arteries and/or uterine arteries, and complete normal ovaries are not presented in CT scans (Table 2).

Univariate analysis results of clinical data, CA-125 level and CT image features

There was no significant difference in age, dysmenorrhea, paramenia and FIGO stage. The presence of clinical symptoms, such as palpable mass, vaginal bleeding and abdominal pain, does not display significant difference between two disease groups. Extrauterine leiomyoma patients has larger proportion of premenopausal individuals, while sex cord-stroma tumor patients are almost evenly distributed into premenopausal and postmenopausal groups. Sex cord-stroma tumor patients have remarkably higher level of serum CEA (p-value=0.0023) and CA-125 (p-value=0.0000).

CT image features of both disease groups did not show significant difference in tumor size, tumor location, morphology, or composition. The tumors of extrauterine leiomyoma and sex cord-stroma tumor are almost equally located in each side of ureters, and a small portion of them occur in both sides of ureters (Table 2). Both disease groups have consistently larger proportion of oval tumors than irregularly shapes ones. Most of the patients in both groups are mixed cystic and solid tumors. Extrauterine leiomyoma tumors are consistently enhanced to a moderate or significant extent after the injection of iopamidol, while only 3 cases of the sex cord-stroma tumors are moderately enhanced (p-value=0.000). Sex cord-stroma tumors were supplied by arteries of ovarian, uterine or both, while none of the extrauterine leiomyoma cases were supplied by ovarian artery (p-value=0.000). None of the sex cord-stroma tumor patients presented normal ovary, and 33/36 had OVPS, and 10/36 has ascites. By contrast, extrauterine leiomyoma only has 8/43 cases with OVPS (p-value=0.000), and 3/43 with ascites (p-value=0.0164).

Multivariate logistic regression analysis of clinical data and CT image features

We then take the variables that demonstrated significant difference between the two disease groups into a multivariate logistic regression model. Results showed that CEA, CA-125 levels, enhancement of mass, arterial blood supply, and presence of normal ovary, OVPS and ascites are independent factors for differentiation of extrauterine leiomyoma and sex-cord stroma tumors (Table 3 & Table 4). ROC curves were then derived to calculate the detective effectiveness of both multivariate logistic models. The AUC was 0.952 for logistic model of extrauterine leiomyoma, with sensitivity of 0.93 and specificity of 0.912, suggesting a remarkable detecting power (Table 5). The multivariate logistic model for sex cord-stroma also demonstrated considerable detecting effectiveness, with AUC of 0.908, specificity of 0.862 and sensitivity of 0.805 (Table 6).

DISCUSSION

Uterine leiomyoma is a common benign tumor in female reproductive system, and 5-10% of them are extrauterine leiomyoma [7, 14]. Extrauterine leiomyoma projects beyond the uterus towards the serosal surface. It is difficult to differentiate from other solid tumors when it grows to occupy the whole pelvic cavity or abdominopelvic cavity [15]. Ovarian sex cord-stromal tumor is a group of tumor composed of sex cord-stroma cells, supporting cells and stroma cells with various degrees of differentiation. It has relatively low incidence but the mortality is high [16]. Ovary is the most delicate organ with the most variety of pathological types, and its imaging presentation is complicated. The variety of organs and intricate anatomical structure of pelvic or abdominopelvic cavity could lead to oppression or metastasis of large tumors, which compound on the difficulties in locating, diagnosis and differentiation of pelvic tumors [17]. Pelvic cavity CT could provide fast scans with high resolution. Alessandrino et al. [18] demonstrated

that CT scans hold huge promise for identifying the source, site of origin, and differentiation of atypical uterine leiomyoma. Lin et al. [19] revealed that CT has advantages in diagnosis of pelvic malignancies and became an effective diagnostic tool.

Both uterus and ovary are intraretroperitoneal viscera located in front or interior of the proximity to ureter. Previous study found that subserous myoma and broad ligament myoma are always located in front of ureter[18]. Tinelli et al. [20] revealed that although sex cord-stromal tumor could oppress the ureter, the relative spatial relation was never changed. The CT axial images used in the present study demonstrated that the relative spatial relation between both extrauterine leiomyoma and sex cord-stroma tumors and ureter are consistent with previous studies [18, 20], suggesting the anatomical area of interest for diagnosis of both diseases. When tumor grows large that obscures adjacent organs or become dislocated, the accuracy of diagnosis based on tissue structure, composition and growth pattern will compromise[21]. Tumor blood vessels usually have larger diameter and are irregularly distributed [22]. Previous studies showed that tumor blood vessels is a direct image sign that can be used to identify origin of tumor [23]. Hu et al. [24] discovered that multi-slice spiral CT vascular 3-dimensional reconstruction technique could reveal the origin of feeding arteries of large tumors, which provides basis for locating the tumor.

The tumors selected for this study have more solid component and are larger in volume, and there is a marked increase of diameter of tumor blood vessels. Our study demonstrated that extrauterine leiomyoma are mainly supplied by uterine arteries which have more branches and evenly distributed within the tumor and 100% enhanced by contrast. On the other hand, sex cord-stroma tumors are predominantly supplied by ovarian arteries which has less branches and evenly distributed within the tumor, but 91.6% enhanced. Around 62.79% extrauterine leiomyoma showed normal ovary tissues, but sex cord-stroma tumor could not present normal ovary. OVPS is characterized by gonadal veins directly join the pelvic mass, which is a CT sign peculiar to ovarian origin tumors [25]. Our study showed that the occurrence of OVPS in sex cord-stroma tumor is significantly higher than extrauterine leiomyoma, indicating that OVPS is a potential CT sign differentiating the two types of tumors. In the present study, we found a swirl sign in the solid portion of extrauterine leiomyoma which is moderately or substantially enhanced, while there is only slight enhancement observed in the sex cord-stroma tumors. Ascites were more frequently observed in sex cord-stroma tumor than in extrauterine leiomyoma.

Pathological ascertainment as gold standard, ROC was drawn based on diagnosis of CT signs and serum CEA and CA-125 levels. Preoperative CT scans combined with serum CEA and CA-125 levels resulted in accuracy of 95.2% in extrauterine leiomyoma (sensitivity=93%, specificity=91.2%), and 90.8% in sex cord-stroma tumor (sensitivity=80.56%, specificity=86.2%). In the recruited subjects, there were 2 cases of broad ligament myoma and 2 cases of ovarian follicular cytoma that rendered vague images of ovaries or blood vessels due to space occupancy and squeezing of large tumors, which led to misdiagnosis. A case of extrauterine leiomyoma was misdiagnosed as ovary origin tumor because the tumor volume was as large as 10cm×15cm and was supplied by both uterine and ovarian arteries. A case of ovarian granulosa cell tumor was misdiagnosed as endometrioid carcinoma due to blood supply by bilateral uterine arteries and absence of OVPS. Two case of ovarian follicular cytoma and a case of ovarian granulosa cell tumor have transformation of cystic into solid tumors and were misdiagnosed as ovarian cystadenoma. A case of ovarian fibroma was misdiagnosed as broad ligament myoma.

Therefore, the characteristics of enhancement, the spatial relation between tumor and adjacent tissue, clinical manifestations and biomarkers such as CEA and CA-125 can facilitate diagnosis when the vessels were not well presented in CT images or the tumors were supplied by both uterine and ovarian artery branches. In addition, ultrasonography and MRI are also encouraged to assist diagnosis. In conclusion, CT scans combined with CEA and CA-125 levels holds promise to serve as diagnostic method for differentiating extrauterine leiomyoma and sex cord-stroma tumor.

REFERENCE

[1] Hori Y, Ito K, Hamamichi S, et al (2017) Functional Characterization of VEGF- And FGF-induced Tumor Blood Vessel Models in Human Cancer Xenografts. Anticancer Res 37:6629–6638. https://doi.org/10.21873/anticanres.12120

[2] Horta M, Cunha TM (2015) Sex cord-stromal tumors of the ovary: a comprehensive review and update for radiologists. Diagn Interv Radiol 21:277–286.

https://doi.org/10.5152/dir.2015.34414

[3] Shah R, McCluggage WG (2017) Unclassifiable malignant extraovarian sex cord-stromal tumors: report of 3 cases and review of extraovarian sex cord-stromal tumors. Int J Gynecol Pathol 36:438–446

[4] Mülayim B (2015) Unaware of a large leiomyoma: A case report with respect to unusual symptoms of large leiomyomas. Ann Med Surg 4:431–433. https://doi.org/https://doi.org/10.1016/j.amsu.2015.09.002

[5] Rozário Garcia FA, Gaigher VP, Neves Ferreira R, Chambô Filho A (2018) Uterine Tumor Resembling Ovarian Sex-Cord Tumors Initially Diagnosed as a Prolapsed Fibroid. Case Rep Obstet Gynecol 2018:

[6] Hubert J, Bergin D (2008) Imaging the female pelvis: When should MRI be considered? Appl Radiol 37:9

[7] Szklaruk J, Tamm EP, Choi H, Varavithya V (2003) MR Imaging of Common and Uncommon Large Pelvic Masses 1. Radiographics 23:403–424. https://doi.org/10.1148/rg.232025089

[8] Stiglmayer R (1978) [Carcinoembryonic antigen in gynecological oncology]. Fortschr Med 96:1843–1845

[9] Brioschi PA, Bischof P, Rapin C, et al (1985) Longitudinal study of CEA and CA125 in ovarian cancer. Gynecol Oncol 21:1–6. https://doi.org/https://doi.org/10.1016/0090-8258(85)90225-2128-134.pdf

[10] Asad-Ur-Rahman F, Saif MW (2016) Elevated Level of Serum Carcinoembryonic Antigen (CEA) and Search for a Malignancy: A Case Report. Cureus 8:e648

[11] Stiekema A, Boldingh QJAJ, Korse CM, et al (2015) Serum human epididymal protein 4 (HE4) as biomarker for the differentiation between epithelial ovarian cancer and ovarian metastases of gastrointestinal origin. Gynecol Oncol 136:562–566. https://doi.org/https://doi.org/10.1016/j.ygyno.2014.12.037

[12] Bai H, Sha G, Xiao M, et al (2016) The prognostic value of pretreatment CA-125 levels and CA-125 normalization in ovarian clear cell carcinoma: a two-academic-institute study. Oncotarget 7:15566–15576. https://doi.org/10.18632/oncotarget.7216

[13] Fiaschetti V, Fornari M, Cama V, et al (2015) MRI in the assessment of prolapsed pedunculated submucous leiomyomas: two case reports. Clin Exp Obstet Gynecol 42:827–832

[14] Mülayim B (2015) Unaware of a large leiomyoma: A case report with respect to unusual symptoms of large leiomyomas. Ann Med Surg 4:431–433. https://doi.org/10.1016/j.amsu.2015.09.002

[15] Schultz KAP, Harris AK, Schneider DT, et al (2016) Ovarian sex cord-stromal tumors. J Oncol Pract 12:940–946. https://doi.org/10.1200/JOP.2016.016261

[16] Borrelli GM, de Mattos LA, Andres M de P, et al (2017) Role of Imaging Tools for the Diagnosis of Borderline Ovarian Tumors: A Systematic Review and Meta-Analysis. J Minim Invasive Gynecol 24:353–363. https://doi.org/10.1016/j.jmig.2016.12.012

[17] Alessandrino F, Dellafiore C, Eshja E, et al (2013) Differential Diagnosis for Female Pelvic Masses. Med Imaging Clin Pract. https://doi.org/10.5772/53139

[18] Lin MY, Dobrotwir A, McNally O, et al (2018) Role of imaging in the routine management of endometrial cancer. Int J Gynecol Obstet 143:109–117. https://doi.org/10.1002/ijgo.12618

[19] Tinelli A, Pellegrino M, Chiuri VE, Malvasi A (2010) Ovarian Sex Cord-Stromal Tumors in Postmenopausal Women and Total Laparoscopical Management. J Cancer Ther 01:31–35. https://doi.org/10.4236/jct.2010.11005

[20] Foo J, Leder K, Mumenthaler SM (2013) Cancer as a moving target: Understanding the composition and rebound growth kinetics of recurrent tumors. Evol Appl 6:54–69. https://doi.org/10.1111/eva.12019

[21] Nagy JA, Chang S-H, Dvorak AM, Dvorak HF (2009) Why are tumour blood vessels abnormal and why is it important to know? Br J Cancer 100:865–869. https://doi.org/10.1038/sj.bjc.6604929

[22] Nishino M, Hayakawa K, Minami M, et al (2003) Primary Retroperitoneal Neoplasms: CT and MR Imaging Findings with Anatomic and Pathologic Diagnostic Clues. Radiographics 23:45–57. https://doi.org/10.1148/rg.231025037

[23] Hu HJ, Huang YW, Zhu YC (2014) Tumor feeding artery reconstruction with multislice spiral CT in the diagnosis of pelvic tumors of unknown origin. Diagnostic Interv Radiol 20:9–16. https://doi.org/10.5152/dir.2013.12176

[24] Lee JH, Jeong YK, Park JK, Hwang JC (2003) "Ovarian vascular pedicle" sign revealing organ

of origin of a pelvic mass lesion on helical CT. Am J Roentgenol 181:131–137. https://doi.org/10.2214/ajr.181.1.1810131

Figures and Tables

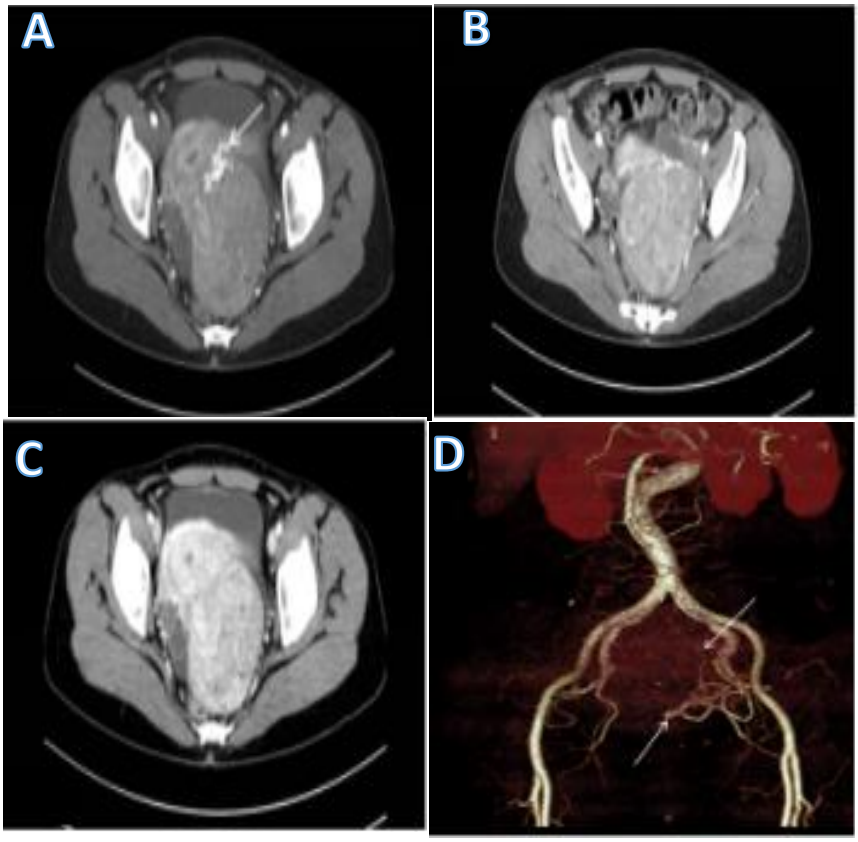

Figure 1. **Extrauterine leiomyoma. Female, 38 years old, subserous myoma on left uterus.**
A: high density CT imaging displayed the walking of vessels, the arteries of left uterus infiltrated into the tumor (white arrows); B: Multiplannar reconstruction tracing of ovaries on both sides demonstrated normal ovary; C: contrast-enhanced CT imaging presented the enhancement of swirl sign in the solid part of the tumor, which bordered on the uterus; D: 3-dimensional volume reconstruction exhibited that the blood vessels are mainly the left uterine arteries.

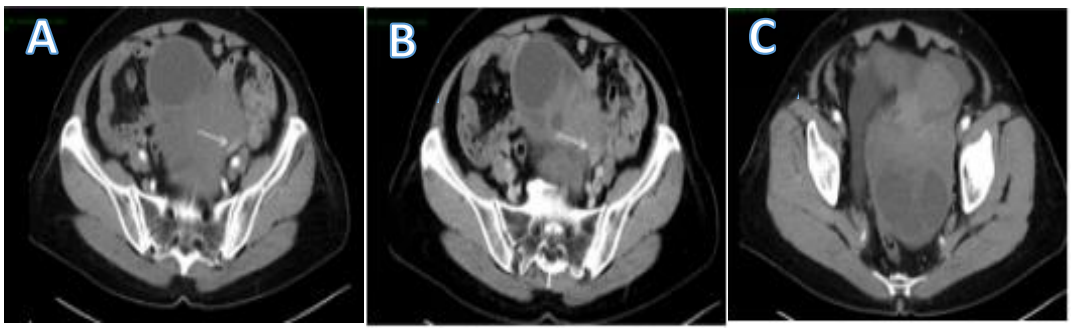

Figure 2. **Sex cord-stroma tumor. Female, 66 years-old, ovarian granulosa-stromal cell tumor (left side).**
A: Axial arterial phase demonstrated that the left ovarian arteries are the major supply vessels (white arrows); B: OVPS can be found in axial arterial phase (white arrows), with tumor slightly enhanced; C: sheet-like ascites in the pelvic.

Table 1. **Clinical characteristics of the two groups**

	Extrauterine leiomyoma (n=43)	Sex cord-stroma tumor (n=36)	P value
Age	44.53±19.78	51.73±9.72	0.0554
Menopausal status			0.0021
Premenopause	34	16	
Post-menopause	9	20	
Dysmenorrhea			1
Negative	5	4	
Positive	38	32	
Paramenia			0.5023
Negative	24	17	
Positive	19	19	
Clinical symptoms			1
Palpable mass	4	4	
Vaginal bleeding	5	4	
Abdominal pain	36	29	
CEA level	1.82	3.11	0.0023
CA125 level	184.42	627.35	0.0000
FIGO Stage			0.7958
I/II	33	26	
III/IV	10	10	

Table 2. **CT imaging findings of both groups**

	Extrauterine leiomyoma (n=43)	Sex cord-stroma tumor (n=36)	P value
Tumor size	115.32±25.87	123.17±37.29	0.3413
Location			0.8545
Left	19	16	
Right	20	15	
Both	4	5	
Morphology			0.5551
Oval	37	29	
Irregularly	6	7	
Composition			1
Mixed cystic-solid	39	32	
Solid	4	4	
Enhancement of solid mass			0
No/slight	0	33	
Moderate/significant	43	3	
Arterial blood supply			0
Ovarian arterial blood supply	0	10	
Uterine arterial blood supply	37	10	
Ovarian and uterine arterial branches blood supply	6	16	
Normal ovary	27	0	0
Presence of OVPS	8	33	0
Presence of ascites	3	10	0.0164

Table 3. **Multivariate logistic regression analysis for prediction of extrauterine leiomyomas**

	B	**SE**	**Wald**	**OR**	**95% CI**	**P value**
CEA	0.327	0.044	8.345	1.387	1.121-1.847	0.006
CA-125	0.456	0.037	9.873	1.593	1.232-2.124	0.002
Enhancement of solid mass	0.762	0.381	20.559	2.143	1.528-4.291	0.001
Arterial blood supply	0.221	0.045	7.835	1.248	1.024-1.523	0.042
Normal ovary	0.419	0.733	6.124	1.521	1.235-2.103	0.002
Presence of OVPS	-1.406	0.121	13.492	0.245	0.062-0.734	0.003
Presence of ascites	-0.860	0.053	10.395	0.423	0.071-0.825	0.002

Table 4. **Multivariate logistic regression analysis for prediction of sex cord-stroma tumor**

	B	**SE**	**Wald**	**OR**	**95% CI**	**P value**
CEA	0.489	0.052	16.273	1.632	1.213-2.241	0.002
CA-125	0.710	0.064	20.452	2.034	1.629-4.253	0.001
Enhancement of solid mass	-0.886	0.073	13.397	0.412	0.145-0.628	0.004
Arterial blood supply	-0.194	0.021	2.024	0.823	0.721-0.953	0.245
Normal ovary	-1.541	0.214	10.487	0.214	0.092-0.848	0.006
Presence of OVPS	1.142	0.176	18.208	3.135	1.735-6.342	0.001
Presence of ascites	0.319	0.025	15.204	1.376	1.121-1.829	0.003

Table 5. **ROC curve values for logistic model predicting extrauterine leiomyomas**

	AUC	**P value**	**95% CI**	**Sensitivity**	**Specificity**
Logistic	0.952	0.000	0.872-0.973	0.930	0.912
CEA	0.735	0.000	0.624-0.892	0.734	0.836
CA-125	0.856	0.000	0.683-0.922	0.897	0.864
Enhancement of solid mass	0.867	0.000	0.725-0.914	0.912	0.851
Arterial blood supply	0.678	0.002	0.573-0.783	0.462	0.584
Normal ovary	0.614	0.003	0.531-0.735	0.635	0.482
Presence of OVPS	0.624	0.042	0.512-0.721	0.513	0.615
Presence of ascites	0.636	0.031	0.538-0.742	0.534	0.556

Table 6. **ROC curve values for logistic model predicting sex cord-stroma tumor**

	AUC	**P value**	**95% CI**	**Sensitivity**	**Specificity**
Logistic	0.908	0.000	0.872-0.973	0.805	0.862
CEA	0.725	0.000	0.634-0.812	0.634	0.736
CA-125	0.872	0.000	0.763-0.945	0.883	0.756
Enhancement of solid mass	0.767	0.000	0.683-0.834	0.635	0.834
Arterial blood supply	0.732	0.003	0.673-0.805	0.836	0.582
Normal ovary	0.631	0.004	0.545-0.722	0.585	0.492
Presence of OVPS	0.612	0.042	0.534-0.689	0.533	0.641
Presence of ascites	0.645	0.025	0.536-0.718	0.568	0.575